Substrate priming enhances phosphorylation by the budding yeast kinases Kin1 and Kin2

Received for publication, August 30, 2018, and in revised form, October 4, 2018 Published, Papers in Press, October 10, 2018, DOI 10.1074/jbc.RA118.005651

Grace R. Jeschke[‡], Hua Jane Lou[‡], Keith Weise[‡], Charlotte I. Hammond[§], Mallory Demonch[¶], Patrick Brennwald[¶], and Benjamin E. Turk[‡1]

From the [‡]Department of Pharmacology, Yale School of Medicine, New Haven, Connecticut 06520, the [§]Department of Biology, Quinnipiac University, Hamden, Connecticut 06518, and the [¶]Department of Cell and Developmental Biology, University of North Carolina, Chapel Hill, North Carolina 27599

Edited by Ronald C. Wek

Multisite phosphorylation of proteins is a common mechanism for signal integration and amplification in eukaryotic signaling networks. Proteins are commonly phosphorylated at multiple sites in an ordered manner, whereby phosphorylation by one kinase primes the substrate by generating a recognition motif for a second kinase. Here we show that substrate priming promotes phosphorylation by *Saccharomyces cerevisiae* Kin1 and Kin2, kinases that regulate cell polarity, exocytosis, and the endoplasmic reticulum (ER) stress response. Kin1/Kin2 phosphorylated substrates within the context of a sequence motif distinct from those of their most closely related kinases. In particular, the rate of phosphorylation of a peptide substrate by Kin1/Kin2 increased >30-fold with incorporation of a phosphoserine residue two residues downstream of the phosphorylation site. Recognition of phosphorylated substrates by Kin1/Kin2 was mediated by a patch of basic residues located in the region of the kinase αC helix. We identified a set of candidate Kin1/Kin2 substrates reported to be dually phosphorylated at sites conforming to the Kin1/Kin2 consensus sequence. One of these proteins, the t-SNARE protein Sec9, was confirmed to be a Kin1/Kin2 substrate both *in vitro* and *in vivo*. Sec9 phosphorylation by Kin1 *in vitro* was enhanced by prior phosphorylation at the +2 position. Recognition of primed substrates was not required for the ability of Kin2 to suppress the growth defect of secretory pathway mutants but was necessary for optimal growth under conditions of ER stress. These results suggest that at least some endogenous protein substrates of Kin1/Kin2 are phosphorylated in a priming-dependent manner.

Given the prevalence of protein phosphorylation as a regulatory mechanism in eukaryotes, it is perhaps not surprising that many proteins are phosphorylated at multiple sites. For example, according to data compiled by the PhosphoSite database, over 5000 human proteins have 10 or more sites of phosphorylation (1). Hierarchical, or ordered, phosphorylation, frequently contributes to this phenomenon (2, 3). A common mechanism for ordered phosphorylation is for a kinase to specifically recognize a phosphorylated residue within its substrates. Such "phosphorecognition" can be mediated by noncatalytic domains in the kinase, such as phosphotyrosine-binding SH2 domains (4) or phosphothreonine-binding forkhead-associated (FHA) domains (5), or by adaptor subunits, such as the cyclin-dependent protein kinase-associated protein Cks1 (6). In addition, there are several kinases that phosphorylate residues in close proximity to prior sites of phosphorylation. The first such kinases to be characterized were glycogen synthase kinase 3 (GSK3)[2] isozymes, which phosphorylate their substrates at sites four residues upstream of a phosphorylated Ser or Thr residue (7). Hierarchical phosphorylation by GSK3 is mediated by specific recognition of phosphorylated amino acids through a patch of basic residues appropriately positioned within the catalytic cleft (8, 9). Several other kinases can recognize substrates primed at specific sites either upstream (casein kinase 1 (CK1)) or downstream (CK2, Cdc7, FAM20C) of their own sites of phosphorylation (2, 10, 11). Although most hierarchical phosphorylation has been ascribed to Ser-Thr kinases, recently several protein Tyr kinases were demonstrated to recognize pTyr-primed substrates (12, 13).

Hierarchical phosphorylation can serve a number of potential functions. It can provide a mechanism for signal integration and cross-talk, because multisite phosphorylation of the substrate depends on activation of both priming and priming-dependent kinases. Dual phosphorylation can promote specific protein–protein interactions. For example, ordered phosphorylation of the adaptor protein Shc by the Tyr kinases Src and epidermal growth factor receptor mediates high affinity binding to the SH2 domain of its effector protein Grb2 (13). Dual phosphorylation of proteins within specific consensus sequences generates so-called phosphodegron motifs that are recognized by specific Skp2-cullin-F-box E3 ubiquitin ligase complexes, thus triggering ubiquitin-dependent proteasomal degradation (14). Finally, clustering of phosphorylation sites

This work was supported by National Institutes of Health Grants R01 GM104047 and R01 GM105947 (to B. E. T.) and R01 GM054712–21 (to P. B.). The authors declare that they have no conflicts of interest with the contents of this article. The content is solely the responsibility of the authors and does not necessarily represent the official views of the National Institutes of Health.

This article contains Tables S1–S3 and Fig. S1.

[1] To whom correspondence should be addressed: Dept. of Pharmacology, Yale School of Medicine, P.O. Box 208066, 333 Cedar St., New Haven, CT 06520. E-mail: ben.turk@yale.edu.

[2] The abbreviations used are: GSK, glycogen synthase kinase; AMPK, AMP-activated protein kinase; CK, casein kinase; ER, endoplasmic reticulum; MARK, microtubule affinity-regulating kinase; MORF, moveable open-reading frame; MRM, multiple reaction monitoring; PSPL, positional scanning peptide library; UPR, unfolded protein response; TAP, tandem affinity purification.

Table 1

Residues positively selected by Kin2 by peptide library analysis

Selectivity values (shown in parentheses for each of two replicates) are quantified peptide array spot intensities normalized such that the average value at a given position is 1. Positively selected residues are shown where the average selectivity value from the two experiments was >2.

Position									
−5	−4	−3	−2	−1	0	+1	+2	+3	+4
Lys (2.0, 2.2)	Trp (2.7, 2.3)	Trp (1.4, 5.0)	Asn (4.7, 10.8)	Xaa	Ser/Thr	pThr (4.0, 2.8)	pThr (10.9, 12.0)	Asn (3.0, 2.4)	Leu (6.6, 7.5)
		His (3.5, 0.7)	Ser (2.5, 2.1)			Thr (2.3, 2.6)		Trp (2.0, 3.3)	Ile (2.4, 3.5)
		Gln (0.7, 3.4)						Asp (2.7, 1.9)	Val (2.9, 2.3)

can have a large impact on local charge, affecting intramolecular interactions, as well as binding to cell membranes or other proteins (15). Such effects can be amplified by "self-priming," in which runs of appropriately spaced sites are phosphorylated in succession (3).

In this study we report that substrate priming promotes phosphorylation by the closely related budding yeast kinases Kin1 and Kin2 (Kin1/2). Kin1/2 are understudied members of a family of Ser-Thr kinases related to AMP-activated protein kinase (AMPK) (16–18). They are most closely related to the microtubule affinity-regulating kinases (MARKs, also called Par-1) in multicellular eukaryotes, sharing an N-terminal kinase catalytic domain, as well as a C-terminal phospholipid-binding kinase-associated 1 domain proposed to promote membrane association (19, 20). Kin1/2 have been implicated in several cellular processes in budding yeast. Both kinases were identified as high-copy suppressors of secretory pathway mutants, functioning to promote exocytic vesicle fusion with the plasma membrane (21). Kin2 function in the secretory pathway appears to require its localization to the periphery of the growing bud (22). Kin2 overexpression causes defects in septin organization, polar hyperaccumulation of cell wall components, and sensitivity to cell wall disrupting agents (22). Although *Saccharomyces cerevisiae kin1*Δ *kin2*Δ double mutant cells have no overt cell polarity defect, deletion of the sole ortholog Kin1 in *Schizosaccharomyces pombe* results in substantial defects in bipolar growth, cell morphology, and organization of the cell wall (23–28). These observations suggest that roles for the kinases in cell polarity are conserved yet more essential to fission yeast. More recently a role for budding yeast Kin1/2 was established in the ER stress-activated unfolded protein response (UPR) (29). Kin1/2 appear to promote processing of the mRNA encoding the ER stress-responsive transcription factor Hac1, and combined deletion of Kin1/2 sensitizes cells to ER stress agents. Whether the functions of Kin1/2 in the UPR and in polarized growth are mechanistically related remains to be determined.

Although a series of Kin1 substrates involved in cell polarity were recently identified through phosphoproteomics studies of fission yeast (30), to date no substrates of budding yeast Kin1/2 have been found. Here, we exploit the priming dependence of Kin1/2 and other features of its substrate phosphorylation motif to identify Sec9 as a direct substrate of the kinases *in vitro* and *in vivo*. By structure-guided mutagenesis, we designed Kin1/2 alleles defective for recognition of phosphorylated substrates, allowing us to examine the importance of substrate priming for their function *in vivo*. We find that substrate priming enhances Kin2 function in the ER stress response yet is dispensable for its role in promoting exocytosis. These studies suggest that recognition of phosphorylated substrates by Kin1/2 may provide a mechanism to confer robustness to cellular stress by optimizing phosphorylation of key substrates.

Results

Kin1 and Kin2 share an unusual phosphorylation consensus sequence including a phosphorylated residue at the +2 position

We recently determined phosphorylation site consensus motifs for 62 *S. cerevisiae* kinases by positional scanning peptide library (PSPL) analysis (31). This analysis included five AMPK-related kinases (Snf1, Gin4, Hsl1, Kcc4, and Kin1). Most of these kinases shared a common consensus motif similar to that previously described for Snf1 and mammalian AMPK (32). This motif includes strong selectivity for hydrophobic aliphatic residues at the −5 and +4 positions relative to the phosphorylation site, as well as an Arg residue at the −3 position (Φ*XBXX*S*XXX*Φ, where Φ is an aliphatic residue, and *B* is a basic residue). Interestingly, Kin1 had a distinct motif that lacked selectivity for basic residues at the −3 position. To determine whether Kin2 shared this unusual motif, we purified the kinase from a yeast overexpression system and performed PSPL analysis (highly selected residues are shown in Table 1, and full quantified data are provided in Table S1). As anticipated based on their high degree of sequence similarity (93% within the catalytic domain), Kin2 had a phosphorylation consensus motif indistinguishable from Kin1. Kin1/2 shared selectivity for an aliphatic hydrophobic residue at the +4 position with other AMPK-related kinases. However, the two kinases had unusual features that diverge from other kinases within the family, including strong selectivity for Asn at the −2 position. Interestingly, Kin1/2 also appeared to strongly prefer pThr at the +2 position, suggesting that their activity is enhanced by priming phosphorylation of substrates. Notably, other kinases that phosphorylate primed substrates are directed by phosphorylation at other positions (2). Kin1/2 thus appeared to have a unique phosphorylation site motif distinct from previously characterized kinases.

To verify the PSPL results, we synthesized a peptide, termed KINtide, that incorporated the residues selected most strongly at the key −2 and +4 positions (Asn and Leu, respectively). The KINtide sequence was derived from the Kin1/2 phosphorylation site in Sec9 (described below). In addition, we synthesized a series of KINtide variants in which specific residues were substituted with Ala, as well as an additional peptide incorporating pSer at the +2 position. Kin1 or Kin2 could phosphorylate the unmodified KINtide *in vitro*, albeit at a modest rate (Fig. 1*A*). Substitution of either the −2 Asn or the +4 Leu for Ala reduced the rate of phosphorylation by Kin1 substantially, confirming

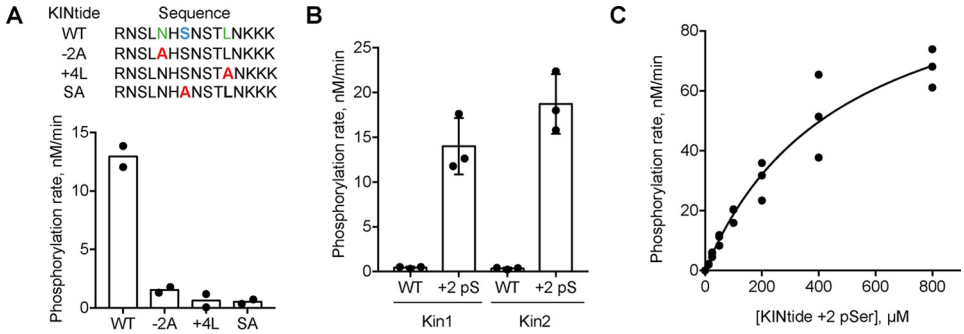

Figure 1. Kin1 and Kin2 preferentially phosphorylated primed peptide substrates. *A*, phosphorylation rates of peptides (500 μM) with the indicated sequences by Kin1 (*bars* show mean and individual data points, $n = 2$). *B*, rates of phosphorylation by Kin1 and Kin2 of KINtide variants (50 μM) with either Ser (WT) or pSer (+2 pS) at the +2 position (*bars* show mean and individual data points, $n = 2$). *C*, rate of Kin1 phosphorylation of varying concentrations of the +2 Ser phosphorylated KINtide substrate (all data points are shown, $n = 3$). The data were fit to the Michaelis–Menten equation using Prism 7.0 (GraphPad).

that these residues are preferred by the kinase. Substitution of the intended phosphorylation site Ser residue reduced phosphorylation by ~24-fold, suggesting that little phosphorylation occurs at other Ser or Thr residues within the KINtide sequence. Strikingly, we found that introduction of a +2 pSer residue into KINtide led a greater than 30-fold increase in phosphorylation efficiency by Kin1 or Kin2 (Fig. 1*B*). Although the high K_m value hampered accurate determination of kinetic parameters, we estimate the K_m value for Kin1 phosphorylation of KINtide +2 pSer to be 490 μM (S.E. = 110 μM; Fig. 1*C*). By contrast, the phosphorylation rate of unmodified KINtide was linear with respect to peptide concentration over a similar range (not shown), indicating a much higher K_m value. These results confirm that Kin1/2 activity is strongly enhanced by priming phosphorylation, at least on a peptide substrate.

Priming enhances phosphorylation of Sec9 by Kin1 and Kin2 in vitro

We searched a list of previously mapped phosphorylation sites compiled from multiple budding yeast phosphoproteomics studies (33) to identify proteins phosphorylated within the stringent Kin1/2 consensus sequence (N*X*pS*X*(S/T)*X*(I/L)). We found 45 occurrences of this motif in the yeast phosphoproteome (Table S2) on 42 proteins. Proteins phosphorylated within the context of this motif were significantly enriched for three gene ontology cellular component terms: site of polarized growth (26%, background frequency 3.9%, $p = 3.3 \times 10^{-5}$), bud (21%, background frequency 3.5%, $p = 0.0015$), and bud neck (19%, background frequency 2.8%, $p = 0.0012$). Because Kin2 is reported to localize to sites of polarized growth, including the bud tip and bud neck, at least some of these proteins may be authentic direct substrates (22). In light of the preference of Kin1/2 for primed substrates, it is notable that 19 of the 45 sites were also reportedly phosphorylated at the downstream Ser or Thr residue within the motif. Among the corresponding proteins was the plasma membrane-associated t-SNARE protein Sec9, which was predicted to be phosphorylated at Ser^{190} by Kin1/2 following priming phosphorylation at Ser^{192}. Overexpression of Kin2 in yeast was previously shown to induce Sec9 phosphorylation (21). However, phosphorylation *in vitro* had been mapped to a distinct residue, Ser^{315}, which did not appear to constitute the major site of phosphorylation *in vivo*. Our observation that Kin1 and Kin2 are priming-dependent provides a potential explanation for this discrepancy, because previous assays of Sec9 phosphorylation *in vitro* used an unprimed substrate.

To test whether Sec9 phosphorylation by Kin1/2 was enhanced by priming phosphorylation, we needed to prepare a recombinant Sec9 substrate highly phosphorylated at Ser^{192}. We noted that Ser^{192} falls within the canonical Snf1/AMPK consensus sequence, suggesting that Snf1 could prime Sec9 for subsequent phosphorylation by Kin1/Kin2 (Fig. 2*A*). To examine priming-dependent phosphorylation, we thus treated recombinant GST-Sec9 purified from *Escherichia coli* with active Snf1 in the presence of cold ATP. GST-Sec9 was then repurified on GSH resin to remove Snf1 and subjected to a radiolabel kinase assay with Kin1 (Fig. 2*B*). We found that although Kin1 did phosphorylate nonprimed Sec9, the level of phosphorylation increased by pretreatment with Snf1. No radiolabel incorporation was seen in the absence of Kin1, indicating that the observed increase in phosphorylation was not attributable to inefficient removal of Snf1 during repurification. To further map sites of phosphorylation by both kinases, we utilized three previously described Sec9 fragments corresponding roughly to the N-terminal (NT1), central (NT2), and C-terminal (CT) thirds of the protein (21). As anticipated, we exclusively observed priming-dependent phosphorylation of the central NT2 fragment harboring Ser^{190} and Ser^{192}. In the context of this fragment, a S190A mutation completely abolished both priming-dependent and priming-independent phosphorylation by Kin1 (Fig. 2*C*). In addition, we observed no priming-dependent phosphorylation of Sec9-NT2-S192A, whereas priming-independent phosphorylation was retained. Phosphate-affinity (Phos-tag) gel analysis confirmed that Snf1 alone stoichiometrically phosphorylated Sec9-NT under these conditions as indicated by mobility shift predominantly to a single, slower-migrating species (Fig. 2*D*). This mobility shift was almost entirely dependent on Ser^{192}. We note that under these conditions that phosphorylation of Sec9-NT2-S190A by Snf1 was reduced by approximately one-third, either because Snf1 can also phosphorylate Ser^{190} or because Snf1 prefers a Ser residue at the −2 position. Nevertheless, this degree of reduction in phosphorylation by Snf1 cannot be responsible for the complete lack of priming-dependent phosphorylation of Sec9-NT2-S190A by Kin1.

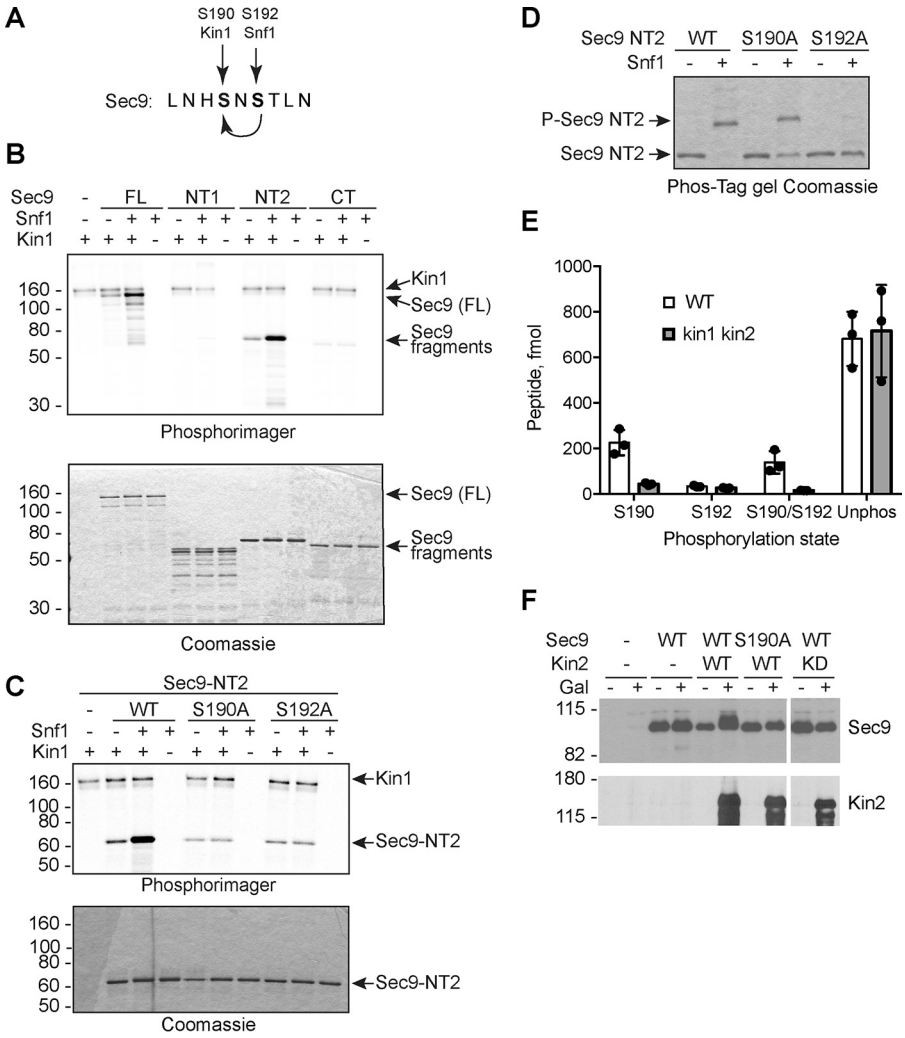

Figure 2. Sec9 is a Kin1/Kin2 substrate *in vitro* and *in vivo*. *A*, scheme showing hierarchical phosphorylation of Sec9 by Snf1 and Kin1. *B*, GST-tagged Sec9 or the indicated fragments were incubated with or without active Snf1 catalytic domain in the presence of ATP and then repurified on GSH resin. Sec9 fragments were then used in Kin1 radiolabel kinase assays, fractionated by SDS-PAGE, and subjected to phosphorimaging. Autophosphorylated Kin1 migrates near the 160-kDa marker. *C*, the Sec9 NT2 fragment (WT or the indicated mutant) was subjected to two-stage Snf1/Kin1 kinase assay as in *B*. *D*, Sec9 NT2 fragments were subjected to phosphorylation by Snf1 catalytic domain and then fractionated by phosphate-affinity SDS-PAGE to separate phosphorylated from nonphosphorylated species followed by Coomassie staining. *E*, full-length Sec9 was immunoprecipitated from cultures of parental or otherwise isogenic *kin1*Δ *kin2*Δ yeast strains. Protein was subjected to SDS-PAGE and Coomassie staining, and the Sec9 gel band was excised, digested with trypsin, and analyzed by MRM LC-MS/MS. Levels of the indicated singly phosphorylated, Ser^{190}/Ser^{192} diphosphorylated, and corresponding nonphosphorylated tryptic peptides were determined using stable isotope-labeled peptide standards. Data points are shown for each biological replicate and represent the average values from all MRM transitions across triplicate MS analysis. *Bars* show means ± S.D. ($n = 3$). *F*, yeast strains harboring a stably integrated galactose-inducible WT or kinase inactive (*KD*) *KIN2* gene were transformed with high-copy number plasmids constitutively expressing Sec9 (WT or the indicated mutant). The cells were grown to midlogarithmic phase in raffinose. Cultures were split and grown an additional 4 h in the presence or absence of 2% galactose as indicated. Protein extracts were prepared, fractionated by SDS-PAGE, and immunoblotted with Sec9 and Kin2 antisera.

Sec9 is a substrate of Kin1 and Kin2 in vivo

To determine whether Sec9 is also phosphorylated *in vivo* by Kin1/2, we performed quantitative MS on overexpressed TAP-tagged Sec9 purified from either WT or *kin1*Δ *kin2*Δ yeast. For these experiments we assessed levels of Sec9 phosphorylation by multiple reaction monitoring (MRM) MS using synthetic, stable isotope-labeled, tryptic peptide standards (34, 35) corresponding to the unphosphorylated species, the Ser^{190}-phosphorylated species, the Ser^{192}-phosphorylated species, or the doubly phosphorylated species. By selecting MRM transitions unique to each peptide, we were able to quantify absolute levels of phosphorylation at Ser^{190} and Ser^{192}, alone or in combination. Purified Sec9 was isolated by SDS-PAGE and digested with trypsin, and phosphopeptides were enriched on a TiO_2 matrix. We analyzed the flowthrough and bound fractions to quantify unphosphorylated and phosphorylated Sec9, respectively (Fig. 2*E*). Levels of both Ser^{190} monophosphorylated and Ser^{190}/Ser^{192} diphosphorylated peptides were dramatically reduced in *kin1*Δ *kin2*Δ cells compared with WT, consistent with Kin1/2 directly phosphorylating Ser^{190} *in vivo*. Levels of the Ser^{190}/Ser^{192} diphosphorylated peptide were ~3-fold higher than the corresponding Ser^{192} monophosphorylated peptide. Although these results are consistent with phosphorylation at Ser^{192} promoting Kin1/Kin2 phosphorylation at Ser^{190}, their interpretation is complicated by the potential for phosphorylation at other sites within the tryptic peptide. In addition, the relative rates of dephosphorylation of the two sites by intracellular phosphatases are unknown. Because Ser^{190} monophosphoryla-

tion is more abundant than Ser^{190}/Ser^{192} diphosphorylation, the majority of Sec9 Ser^{190} phosphorylation *in vivo* may occur independently of substrate priming.

Overexpression of Kin2 in yeast induces Sec9 to undergo an electrophoretic mobility shift caused by phosphorylation at unknown sites (21). We examined the mobility of WT Sec9 and Sec9-S190A by SDS-PAGE upon expression of Kin2 under control of a galactose-inducible promoter. As reported previously, we observed a Sec9 mobility shift in the presence of galactose in the Kin2-expressing strain (Fig. 2*F*). This mobility shift was largely absent for Sec9-S190A, although we did observe a residual mobility shift suggestive of other Kin2-dependent sites of phosphorylation. Taken together with our MS data, these results indicate that Kin2 (and possibly Kin1) can phosphorylate Sec9 at Ser^{190} *in vivo*.

Recognition of primed substrates is mediated by a cluster of basic residues in the N-terminal lobe of Kin1/2

To examine the functional importance of substrate priming by Kin1/2, we sought to generate mutant kinases specifically deficient for priming-dependent phosphorylation. To understand the structural basis for recognition of primed substrates by Kin1/2, we examined the published X-ray crystal structure of human MARK2 in complex with a pseudosubstrate inhibitor, the *Helicobacter pylori* CagA protein (36). We chose this structure because MARK2 is the kinase most similar to Kin1/2 (58% similarity within the catalytic domain) to have been crystallized in complex with a peptide substrate or pseudosubstrate. In this structure, the side chain of the +2 residue is oriented toward the kinase αC helix, a conserved element of the protein kinase fold (Fig. 3*A*). Although MARK2 itself is not priming-dependent (37), multiple sequence alignment with fungal Kin1 homologs revealed a conserved cluster of basic residues spanning the N terminus of the helix αC that are predicted to be oriented toward the +2 residue (Fig. 3*A*). To examine whether these basic residues might be involved in recognition of primed substrates by Kin1, we mutated each of them individually to Ala and assayed these mutants for phosphorylation of the KINtide and KINtide +2 pSer substrates. Individual mutation of Lys^{183}, Arg^{187}, or Arg^{190} each reduced the phosphorylation rate of KINtide +2 pSer relative to the unmodified peptide, with Arg^{187} mutation having the largest effect (Fig. 3*B*). Mutation of Arg^{190} alone reduced phosphorylation of unmodified KINtide by ~2-fold, suggesting that it may be important for kinase activity independent of the substrate used. The combination mutant Kin1-K183A,R187A specifically reduced the rate of phosphorylation of the primed peptide substrate by more than 60-fold with no effect on the phosphorylation rate of unprimed KINtide. The analogous Kin2 mutant (K162A,R166A) behaved similarly (Fig. 3*C*). In addition to affecting priming-dependent phosphorylation of the peptide substrates, Kin1-K183A,R187A was also specifically impaired for Snf1 priming-dependent phosphorylation of the Sec9 NT2 protein fragment (Fig. 3*D*). PSPL analysis of Kin1-K183A,R187A and Kin2-K162A,R166A compared with their WT counterparts showed that these mutations only affected selectivity for phosphorylated residues and did not affect recognition of key residues selected at other positions (Fig. 4 and Table S1). These results indicate that Lys^{183} and

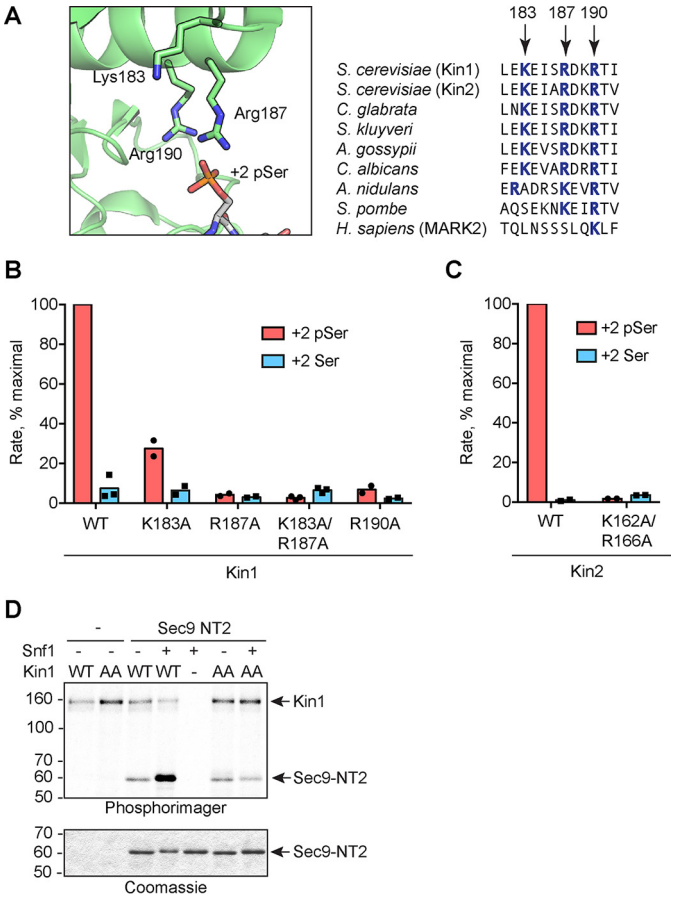

Figure 3. Recognition of phosphorylated residues by Kin1/Kin2. *A*, Kin1-phosphopeptide model (*left panel*) is based on the reported X-ray crystal structure of MARK2 in complex with the CagA pseudosubstrate peptide (Protein Data Bank code 3IEC) (36). MARK2 residues were changed to those at the equivalent position in yeast Kin1 orthologs (*right panel*, *S. cerevisiae* numbering), and the +2 residue in CagA was changed to pSer using the mutagenesis wizard function in PyMOL. *B*, impact of +2 pSer on KINtide phosphorylation by Kin1 β3-αC loop region mutants. Rates are normalized to that of the WT kinase on the +2 pSer peptide (*bars* show mean and individual data points, $n = 3$ for WT and K183A/R187A mutant and $n = 2$ for all others). *C*, relative rates of phosphorylation of KINtide and KINtide +2 pSer by WT Kin2 and Kin2-K162A,R166A normalized as in *B* ($n = 2$). *D*, Snf1-primed Sec9-NT2 fragment was purified and subjected to radiolabel kinase assay with WT Kin1 or Kin1-K183A,R187A (*AA*) as in Fig. 2.

Arg^{187} of Kin1 (and Lys^{162} and Arg^{166} of Kin2) are essential for recognition of primed substrates yet dispensable for phosphorylation of nonprimed substrates.

Priming-dependent Sec9 phosphorylation is not required for Kin1 and Kin2 regulation of the late secretory pathway

Kin1 and Kin2 were previously identified as high-copy suppressors of temperature-sensitive mutants of components of the late secretory pathway, acting upstream of Sec9 (21). We examined the ability of Kin2-K162A,R166A to support growth of several mutants in this pathway at their restrictive temperatures (Fig. 5*A*). We found that the priming defective Kin2 mutant was equal to WT Kin2 in its ability to suppress the temperature-sensitive growth phenotype of all mutants tested. Consistent with our results indicating that Sec9 phosphorylation by Kin1 and Kin2 *in vivo* is largely priming-independent, these experiments suggest that substrate priming is not required for Kin2 function in exocytosis in general, at least

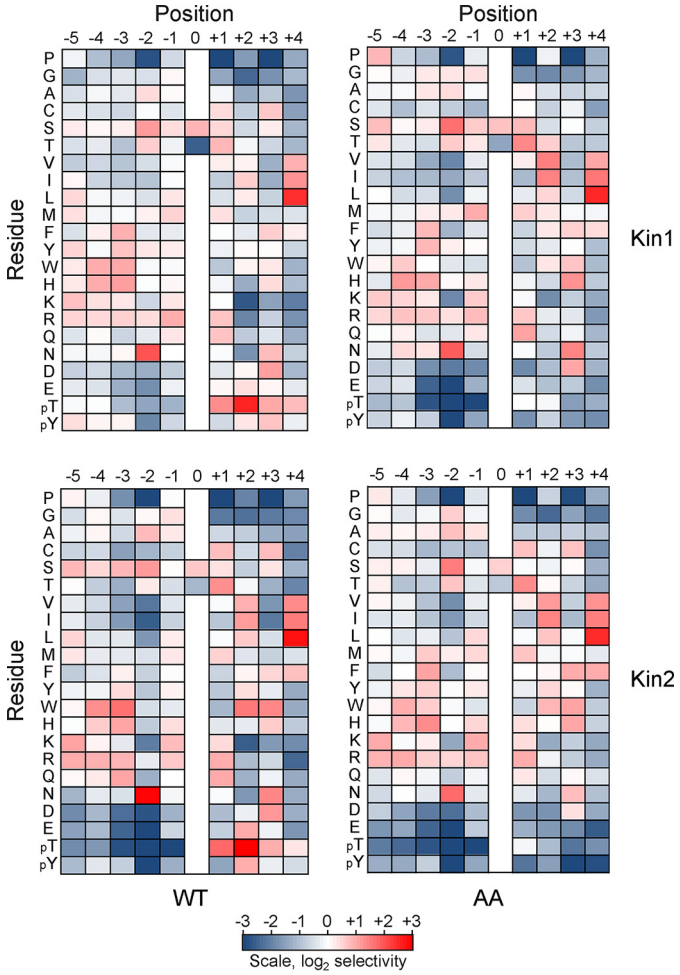

Figure 4. Peptide library analysis of Kin1 and Kin2 priming defective mutants. Heat maps show quantified peptide library analysis of WT and priming-deficient mutant (*AA*) forms of Kin1 and Kin2. Selectivity values are the average of normalized data from two separate experiments. Heat maps were generated in Microsoft Excel.

when overexpressed. These results further confirm that mutation of Lys^{162} and Arg^{166} does not generally inactivate Kin2. We also found that mutation of Ser^{190}, Ser^{192}, and Ser^{315}, alone or in combination, had no effect on the ability of overexpressed Sec9 to suppress growth defects of the same panel of mutants (Fig. S1). These results suggest that phosphorylation by Kin1/2 is not required for Sec9 function when overexpressed.

Priming-defective Kin1 and Kin2 mutants are selectively impaired for function in vivo

Examination of Kin1/2 function in exocytosis requires overexpression, which may bypass a requirement for substrate priming simply by elevating levels of kinase activity. To further investigate potential roles for substrate priming by endogenous Kin1/2, we examined their function in the UPR. As previously reported (29, 38), we found that *kin2*Δ cells grew more slowly than WT cells on medium containing tunicamycin and that combined deletion of *KIN1* and *KIN2* rendered cells highly tunicamycin-sensitive (Fig. 5*B*). Double mutant cells re-expressing Kin2-K162A,R166A from a low-copy plasmid under control of its own promoter grew at a slower rate than those expressing WT Kin2, an effect that was exacerbated at higher concentrations of tunicamycin (Fig. 5, *C* and *D*). We note that in these experiments *kin1*Δ *kin2*Δ cells re-expressing WT Kin2 grew faster on medium containing tunicamycin than corresponding WT cells transformed with a control plasmid, an effect likely mediated by modest overexpression of Kin2 from the expression plasmid. Nonetheless, these results suggest that substrate priming is required for optimal activity of Kin2 in cells in mediating resistance to ER stress.

Discussion

Here, we have shown that phosphorylation by Kin1/2 is strongly promoted by substrate priming. Recognition of pSer or pThr at the +2 position in substrates is mediated by a patch of basic residues in a region comprising a portion of helix αC and the αC–β3 loop. Basic residues in helix αC appear to contribute, at least in part, to recognition of primed substrates by other kinases. However, differences in the precise location and quantity of these basic residues likely underlie the positional specificity of phosphosubstrate recognition. For example, CK2 has a cluster of four basic residues located within helix αC, as well as three additional basic residues within its activation loop. The highly positive net local charge in CK2 is likely responsible for the strong selectivity of CK2 for acidic and phosphorylated residues at both the +1 and +3 positions and to a lesser extent at other downstream positions (39). In contrast Kin1/2 have a limited number of basic residues in this region, correlating with specificity for only a single phosphorylated residue. The +4 pSer-binding site of GSK3 isozymes includes an Arg residue located at the N terminus of helix αC yet includes additional basic residues in the kinase activation loop and catalytic loop. The distinct arrangement of these residues compared with Kin1/2 likely underlies GSK3 selectivity for phosphorylated residues at the +4 rather than the +2 position.

To date the only other kinase reportedly primed by phosphorylation at the +2 position is Golgi casein kinase, recently identified as the secreted protein FAM20C (11, 40). Although FAM20C has some catalytic residues in common with canonical eukaryotic protein kinases, the overall topology of its catalytic domain is distinct (41). The X-ray crystal structure of *Caenorhabditis elegans* FAM20C suggests that substrates bind in a different mode or orientation compared with other kinases. Accordingly, basic residues implicated in recognition of phosphorylated substrates are located distal from helix α6, which is analogous to αC of other eukaryotic protein kinases.

In addition to uniquely recognizing primed substrates, Kin1/2 are also unusual among members of the AMPK family in other aspects of substrate recognition. Members of the calmodulin-dependent protein kinase group to which the AMPK family belongs are typically characterized as "basophilic," essentially requiring an Arg or Lys residue at the −3 position in substrates (2). Kin1/2 by contrast are largely nonselective at this position, likely attributable to a Glu to Gln substitution in a residue important for selecting basic residues (Gln^{230}/Gln^{209} in Kin1 and Kin2, respectively) (31). Kin1/2 are also unique within the family in selecting an Asn residue at the −2 position, a preference it shares with polo-like kinases despite sharing little sequence similarity. Aside from these differences, Kin1/2 are similar to other members of the yeast and

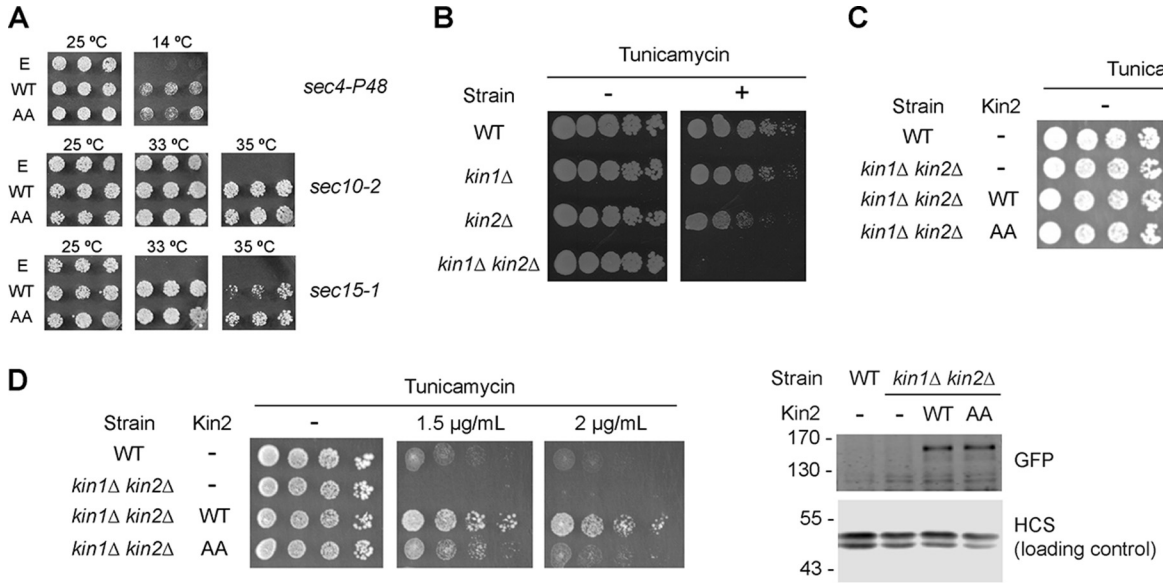

Figure 5. Substrate priming selectively promotes Kin2 function. *A*, cultures of the indicated strains transformed with high-copy plasmids expressing untagged WT Kin2, Kin2-K162A,R166A (*AA*), or the empty vector (*E*) were serially diluted and spotted onto solid YPD medium. The plates were grown at either the permissive (25 °C) or restrictive temperatures (14 °C for *sec4-P48* and 33 or 35 °C for all other strains). *B*, serial 5-fold dilutions of cultures of strain BY4741 (WT) or otherwise isogenic strains of the indicated genotype were spotted onto solid YPD medium in the presence or absence of 0.5 μg/ml tunicamycin. The plates were incubated at 30 °C until WT colonies were visible. *C*, BY4741 (WT) or otherwise isogenic *kin1*Δ *kin2*Δ strains were transformed with a low-copy plasmid expressing GFP fused to WT Kin2 or Kin2-K162A,R166A. The cultures were grown in selective medium, and then serial 5-fold dilutions were plated onto solid SD-Ura medium in the presence or absence of 0.5 μg/ml tunicamycin and grown for 72 h at 30 C. *D*, serial dilutions of cultures were grown as for *C*, but at the indicated concentrations of tunicamycin. Protein was extracted from aliquots of the liquid culture and immunoblotted with antibodies to GFP to determine levels of GFP-Kin2. Homocitrate synthase (*HCS*) served as a loading control.

mammalian AMPK families in having a substantial preference for a Leu residue at the +4 position. In the MARK2-CagA co-crystal structure, the +4 Leu residue of the pseudosubstrate occupies a hydrophobic cavity analogous to the +1 residue-binding site in other kinases. Accommodation of the +4 Leu residue by MARK2 is facilitated by the presence of a small Ala residue immediately upstream of the conserved APE motif at the C terminus of the kinase activation loop (the APE −1 residue). Notably, an Ala residue at the analogous position is found in Kin1/2 and all other members of the AMPK/Snf1 family, explaining their common selectivity at the +4 position. Although mammalian MARKs are not dependent on substrate priming, it is notable they can be phosphorylated at sites in the N terminus of helix αC, which has been reported both to activate (42) and inactivate (43) the kinases. Given the importance of this region in substrate recognition, it is tempting to speculate that its phosphorylation serves to change MARK substrate specificity rather than overall catalytic activity.

Guided by the Kin1/2 phosphorylation site motif, we identified the exocytic t-SNARE protein Sec9 as a direct substrate of the kinases. Previously, Kin1/2 were found to induce Sec9 phosphorylation and dissociation from the plasma membrane, promoting its activity in exocytosis (21). Because mutation of sites phosphorylated by Kin2 *in vitro* had no effect on its phosphorylation in cells, it was concluded that Kin1/2 likely acted indirectly to induce phosphorylation of Sec9. Here, we identified Ser^{190} of Sec9 as a Kin1/2 phosphorylation site that *in vitro* was largely dependent on prior phosphorylation at Ser^{192}. Quantitative analysis confirmed that Sec9 phosphorylation at Ser^{190} phosphorylation depended on Kin1/2 in yeast, albeit in a manner likely independent of Ser^{192} priming. Notably, the Sec9 was not phosphorylated at Ser^{190} to full stoichiometry, and it is possible that stimuli activating the relevant Ser^{192} kinase(s) would enhance Ser^{190} phosphorylation as well. Although Snf1 could phosphorylate Ser^{192} *in vitro*, we found no increase in Ser^{192} or Ser^{190} phosphorylation upon glucose withdrawal (data not shown), conditions that strongly activate Snf1 in yeast. Ser^{192} may therefore be phosphorylated by a distinct kinase with similar substrate specificity, perhaps within the yeast Snf1/AMPK family. We also note that mutation of the Kin1/2 phosphorylation sites in Sec9 did not apparently affect its function in the secretory pathway, at least when overexpressed. Although these experiments may reflect a consequence of overexpression, because *kin1*Δ *kin2*Δ strains have no overt secretory pathway defect, phosphorylation of Sec9 is unlikely to be essential for function. Similarly, we do not believe that phosphorylation of Sec9 is relevant to the function of Kin1/2 in the UPR. Neither overexpression of Sec9 nor low-copy expression of the phosphomimetic mutant Sec9-S190E,S192E could bypass the requirement for Kin1/2 in supporting growth in the presence of tunicamycin.[3] Kin1/2 may therefore promote Sec9 function in other contexts that have yet to be identified.

Using a mutant defective for recognition of primed substrates, we found that priming dependence enhanced the ability of Kin2 to function in the ER stress response, particularly at high concentrations of tunicamycin. These observations suggest that substrates important for Kin1/2 function in the UPR are at least partly dependent on priming for optimal phosphorylation. A possible explanation would be that low-level phos-

[3] G. R. Jeschke, H. J. Lou, and B. E. Turk, unpublished results.

phorylation of a key Kin1/2 substrate is sufficient to withstand mild ER stress but that increased phosphorylation mediated by priming is required at high levels of tunicamycin. Alternatively, increased Kin1/2 activity conferred by substrate priming might be required to counteract phosphatases activated under conditions of severe ER stress. In other systems, an optimal phosphorylation site sequence is not required for a kinase to achieve a high level of substrate phosphorylation *in vivo*. Rather, the presence of a "high quality" phosphorylation site appears to confer robustness to perturbation, for example by requiring lower levels of kinase activation (2). Consequently, some, but not all, substrates of a kinase tend to conform to optimal consensus sequences. Accordingly, it is almost certainly the case that additional Kin1/2 substrates exist aside from those harboring precise matches to their consensus sequence (as listed in Table S2).

Prior studies have suggested that Kin1/2 function in the UPR, as well as in cell polarity and polarized growth. The lack of overt cell polarity defects in *kin1*Δ *kin2*Δ cells may reflect compensation by other, perhaps related, kinases. However, the distinct phosphorylation site motif of Kin1/2 compared with their most closely related kinases suggests that they are likely to have unique roles in cell polarity. Consistent with this notion, Kin2 reportedly localizes to sites of polarized growth in budded cells (22), and a significant fraction of our potential Kin1/2 substrates share this pattern of localization (Table S2). Whether the function of Kin1/2 in cell polarity and cell wall maintenance is related to their roles in the UPR is not clear. Notably, ER homeostasis mediated by components of the UPR pathway is essential for proper organization of the cell wall (44). Furthermore, cell wall–disrupting agents activate the UPR and induce Hac1 mRNA splicing, a Kin1/2-dependent process. Because some of our candidate Kin1/2 substrates modulate sensitivity to tunicamycin and/or cell wall stress (Table S2), it is tempting to speculate that these substrates may contribute to Kin1/2 function in these processes. Future studies will be aimed at verifying these proteins as substrates and investigating the functional impact of their phosphorylation by Kin1/2.

Experimental procedures

Plasmids

Yeast high-copy plasmids (pBG1805) expressing C-terminally tandem affinity purification (TAP)–tagged full-length Kin1, Kin2, and Sec9 from a galactose-inducible promoter were from the movable ORF (MORF) collection and were obtained from the laboratory of Michael Snyder (45). The yeast high-copy plasmids expressing Kin2 and Sec9 from their respective promoters and bacterial expression plasmids for GST-tagged Sec9 fragments and Snf1 catalytic domain (Snf1-cat) were previously described (21, 46, 47). Sec9 fragments corresponded to the following residues: NT1, 1–150; NT2, 166–401; and CT, 402–651. The bacterial expression vector for GST-tagged full-length Sec9 was generated by PCR amplification of the Sec9 coding sequence from the MORF plasmid and insertion into the BamHI and NotI sites of pGEX-4T2. The low-copy vector for expressing GFP-Kin2 from its own promoter (pRS416-GFP-Kin2) included the entire Kin2 ORF plus 1 kb upstream and 250 bp downstream yeast genomic sequence, with yeast codon optimized GFP (from pKT0209, generated by the Kurt Thorn laboratory and obtained from Addgene) inserted between the promoter and the translation start site. All mutants were generated using the QuikChange protocol (Stratagene).

Yeast strains and media

Single deletion mutants on the BY4741 (S288c) genetic background were purchased from Open Biosystems. The *kin1*Δ *kin2*Δ strain (BTY008) was generated by transforming *kin1*Δ cells with a previously described targeting construct including the *LEU2* gene flanked by genomic *KIN2* sequence (18). Clones were selected on SC-Leu medium, and correct targeting of the *KIN2* locus was confirmed by PCR from genomic DNA using primers flanking both ends of the insertion site. Temperature-sensitive secretory pathway mutant strains and strains expressing Kin2 from an integrated galactose-inducible cassette were previously described (21). The host strain for expression of MORF constructs (Y258) was obtained from Michael Snyder. Yeast medium components were from BD Biosciences except for complete supplement dropout mixtures (MP Biomedicals).

Protein expression and purification

TAP-tagged full-length Kin1 and Kin2 used for *in vitro* kinase assays were overexpressed in yeast and purified as described (45) with the following modifications. Yeast (strain Y258) transformed with pBG1805-Kin1 or Kin2 were grown overnight at 30 °C in SD-Ura medium. Cultures were expanded into 400 ml of SC-Ura + 2% raffinose, grown ~16 h to midlogarithmic phase (A_{600} = 0.6–0.7), and induced by adding 200 ml of 3× YEP-Gal medium (3% yeast extract, 6% peptone, 6% galactose). After shaking 6 h at 30 °C, the cells were collected by centrifugation and washed twice with double-distilled H_2O, and pellets were frozen at −80 °C. The cell pellets were thawed on ice, suspended in 2 ml of lysis buffer (50 mM Tris, pH 7.5, 1 mM EDTA, 1 mM EGTA, 0.1% Triton X-100, 1 mM DTT, 0.4 mM Na_3VO_4, 1 mM NaF, 5 mM β-glycerophosphate, 1 mM phenylmethylsulfonyl fluoride, 10 μg/ml aprotinin, 10 μg/ml leupeptin, 2 μg/ml pepstatin A, 10% glycerol) containing 150 mM NaCl and an equal volume of acid-washed 0.5-mm glass beads (Biospec) and lysed by vortexing. Following centrifugation, the supernatant was reserved, and insoluble debris was re-extracted by vortexing in 2 ml of lysis buffer containing 650 mM NaCl. The glass beads were pelleted, and the combined supernatants were diluted with 9 ml of lysis buffer. After adding 100 μl of IgG-Sepharose beads (GE Life Sciences), the slurry was tumbled for 2 h at 4 °C. The beads were pelleted and washed three times with wash buffer (50 mM Tris, pH 7.5, 150 mM NaCl, 0.1% Triton X-100, 10% glycerol) and three times with cleavage buffer (50 mM HEPES, pH 7.4, 150 mM NaCl, 1 mM DTT, 0.1% Tween 20, 25% glycerol). Kinase was released from the beads by overnight treatment with GST-3C protease in 300 μl of cleavage buffer. Following centrifugation, the supernatant was incubated with GSH-Sepharose 4B (GE Life Sciences) to remove the protease. Kinase preparations were snap-frozen in aliquots and stored at −80 °C.

E. coli strains Rosetta (DE3) (for expression of full-length Sec9) or BL21(DE3) (for all other constructs) were purchased from EMD Millipore. Transformed cells were grown at 37 °C to

an A_{600} of 0.8–1.0 in 200 ml of terrific broth with ampicillin, and expression was induced with 0.2 mM isopropyl β-D-thiogalactopyranoside. After 2 h, the cells were pelleted, washed once with cold PBS, and frozen in dry ice/EtOH. Pellets were thawed on ice and resuspended in 5 ml of 20 mM Tris, pH 7.5, 140 mM NaCl, 1 mM EDTA, 1 mM DTT, 10 μg/ml leupeptin with 0.2 mg/ml lysozyme. After 15 min of incubation on ice, 70 μl of 10% sodium deoxycholate and 25 μl of 200 mM phenylmethylsulfonyl fluoride were added and rotated 15 min at ambient temperature. DNase I (150 units) and 65 μl of 1 M $MgCl_2$ were added, and mixing was continued for another 15 min. Insoluble material was removed by centrifugation, and the supernatant was incubated with 0.25 ml of GSH-Sepharose 4B resin with rotation for 1–2 h, 4 °C). The beads were washed three times with GSH wash buffer (50 mM Tris, pH 8.0, 50 mM NaCl, 1 mM DTT, 0.01% Igepal CA630, 10% glycerol). Sec9 constructs were eluted into 0.5 ml of GSH wash buffer containing 10 mg/ml reduced GSH, and eluates were dialyzed overnight at 4 °C into GSH wash buffer. Snf1-cat was cleaved from the GST moiety rotating the beads overnight in 0.25 ml of GSH wash buffer containing 1 unit of thrombin, 2.5 mM $CaCl_2$, and 5 mM $MgCl_2$. Following centrifugation and removal of the supernatant, the beads were incubated with an addition 0.25 ml of GSH wash buffer with rotating for 15 min. The beads were pelleted, and the combined supernatants were incubated with benzamidine-agarose (Sigma–Aldrich) to remove thrombin. The protein samples were aliquoted, frozen in dry ice/EtOH, and stored at −80 °C.

PSPL analysis

Phosphorylation sequence specificity of WT and mutant Kin1 and Kin2 was determined by PSPL analysis (31). The peptide library (Anaspec) consisted of 200 peptide mixtures having the general sequence YA*XXXXX*(S/T)*XXXX*AGKK(biotin), where eight of the nine residues indicated by *X* were an equimolar mixture of the 17 amino acids (excluding Cys, Ser, and Thr), where "S/T" indicates an equimolar mixture of Ser and Thr, and where the biotin group was conjugated to the C-terminal Lys side chain via an aminohexanoic acid spacer. The remaining *X* position was fixed as one of the 20 unmodified amino acid residues, pThr, or pTyr. Kinase reactions (2 μl) were performed in 1536-well plates in kinase assay buffer (50 mM HEPES, pH 7.4, 10 mM $MgCl_2$, 1 mM DTT, 0.1% Tween 20) containing 50 μM peptide substrate, and 50 μM ATP containing 0.03 μCi/ml [γ-^{33}P]ATP (PerkinElmer Life Sciences). Following incubation at 30 °C for 2 h, 200-nl aliquots of each reaction were transferred to a streptavidin-coated membrane (Promega), which was washed and dried as described (31). Radiolabel incorporation into peptides was quantified by phosphorimaging. The data were normalized so that the average signal for the 20 unmodified amino acids at a given position was assigned to 1, and results show the means of two separate runs. Heat maps were generated using Microsoft Excel. Candidate substrates were identified from published phosphoproteomics studies (33) that conformed to the consensus sequence N*X*(pS/pT)*X*-S*X*(I/L). Gene Ontology (GO) term enrichment among the resulting 42 genes was performed using the Saccharomyces Genome Database GO term finder tool (version 0.86) (48).

In vitro kinase assays

Kinase substrate peptides (KINtides) were prepared by standard Fmoc (*N*-(9-fluorenyl)methoxycarbonyl) solid-phase synthesis procedures and purified by reversed-phase HPLC prior to use. Peptide identity was verified by MALDI-MS. Peptide kinase assays were performed in 75 μl of kinase assay buffer containing the indicated concentration of peptide and were initiated by adding ATP to 50 μM (with 0.08 μCi/ml [γ-^{33}P]ATP) and transferring to 30 °C. Aliquots (20 μl) were removed at 5-min intervals and spotted onto P81 phosphocellulose filters (GE Healthcare), which were immediately quenched in 75 mM phosphoric acid. Filters were washed three times in the same solution, air-dried, and analyzed by scintillation counting. Phosphate incorporation into peptides was calculated from standards consisting of varying amounts of reaction mixtures spotted onto filters that were left unwashed. The K_m value was estimated by fitting reaction rates at varying substrate concentration to the Michaelis–Menten equation using Prism 7 (GraphPad software).

To perform *in vitro* priming assays, Snf1-cat (6 μg) was initially activated by incubating with recombinant Elm1 (49) in 30 μl of Snf1 activation buffer (50 mM Tris, pH 8.0, 50 mM NaCl, 10 mM $MgCl_2$, 0.01% Igepal CA-630, 1 mM DTT, 1 mM ATP, 10% glycerol) for 1 h at 30 °C alongside control reactions lacking Snf1. Snf1 reactions were then diluted 10-fold into 75 μl of 10 mM HEPES, pH 7.4, 100 mM NaCl, 10 mM $MgCl_2$, 1 mM DTT, 0.2 mM benzamidine, 1 mM ATP containing 7 μg of GST-Sec9 (full-length or fragment) and incubated 30 min at 30 °C. To purify phosphorylated Sec9, reaction tubes were chilled on ice and diluted with 100 μl of GSH wash buffer (50 mM Tris, pH 8.0, 100 mM NaCl, 1 mM DTT, 0.01% Igepal CA-630) containing 25 μl of GSH-Sepharose beads. After rotating 1 h at 4 °C, the beads were pelleted and washed three times with 0.5 ml of GSH wash buffer. GST fusion proteins were eluted with 35 μl of 6 mg/ml reduced GSH in GSH wash buffer. A portion of the repurified GST fusion proteins were retained for nonradioactive SDS-PAGE. For the second stage of the assay, 10 μl of repurified GST fusion protein was diluted 2-fold into kinase assay buffer containing ~5 ng of Kin1 and 10 μM ATP with 0.1 μCi/μl [γ-^{33}P]ATP and incubated a further 30 min at 30 °C. The reactions were quenched by adding 4 μl of 6× SDS-PAGE loading buffer (final concentrations: 2% SDS, 25 mM Tris, pH 6.8, 10% glycerol, 5% β-mercaptoethanol) and heating to 95 °C for 5 min. The samples were fractionated by SDS-PAGE (10% acrylamide), and gels were stained with Coomassie Blue, destained, dried, and exposed to a phosphor storage screen to detect radiolabel incorporation. Nonradioactive samples were fractionated by Phos-tag SDS-PAGE (containing 7.5% acrylamide, 2.5 μM Phos-tag acrylamide (Wako Chemicals), 5 μM $MnCl_2$), and gels were stained with Coomassie Blue.

Analysis of Sec9 phosphorylation in vivo

Sec9-TAP was expressed in 100-ml cultures of the indicated strains and purified on IgG-Sepharose (25 μl) as described above for Kin1/2-TAP, except that protein was eluted by suspending in 50 μl of 50 mM Tris, pH 6.8 with 1% SDS and heating to 95 °C for 2 min. The beads were centrifuged, and the super-

natant was added to 10 μl of 4× SDS-PAGE loading buffer and reheated. The samples were fractionated by SDS-PAGE (7.5% acrylamide), stained with Coomassie Blue, and destained. The Sec9 band was excised from the gel and submitted to the Yale Keck Biotechnology laboratory for trypsin digestion and MS analysis. Phosphopeptides were enriched from tryptic digests on a TiO_2 matrix. Chemically synthesized, stable isotope-labeled peptides corresponding to the unphosphorylated Ser^{190} and Ser^{192} singly phosphorylated, and Ser^{190}/Ser^{192} doubly phosphorylated tryptic fragment of Sec9 (NSLNHSNSTLNV*GPSR, where V* indicates $^{13}C_5$,$^{15}N_1$-valine, and phosphorylation sites are underlined) were added to aliquots of both the phosphopeptide-enriched fraction and the flowthrough fraction. The samples were subjected in triplicate to MS on an AB Sciex 5500 QTRAP triple quadrupole instrument interfaced with a Waters nanoAcuity UPLC system in MRM mode. MRM spectra were quantified using Multiquant 2.0 software using transitions and peptide retention times previously defined using the synthetic peptides on an LTQ Orbitrap VELOS equipped with the same UPLC system. The following fragment ions were used for the indicated peptides: unphosphorylated, b_{10} and y_4; $pSer^{190}$, b_7 and b_7-H_3PO_4; $pSer^{192}$, b_7 and y_{10}-H_3PO_4; $pSer^{190}$/$pSer^{192}$, y_4. The average signals from all transitions were used for quantification. The data show the averages of three biological replicates. Full MS data for all transitions used for quantification are provided in Table S3.

To examine Sec9 phosphorylation by electrophoretic mobility shift, strains harboring the indicated *KIN2* alleles under control of a galactose-inducible promoter and transformed with pRS426-Sec9 were grown to midlogarithmic phase in SC-Ura containing 3% raffinose. Cultures were then divided in two, and galactose was added to 1% final concentration to one portion. After incubation at 25 °C for 4 h, 5 A_{600} units of each culture were pelleted, washed once with 50 mM Tris, pH 7.4, and snap-frozen in a dry ice-EtOH slurry. Cell extracts were made by adding 200 μl of glass beads and 50 μl of 2% SDS to the frozen pellet, followed by agitation on a vortexing mixer for 2 min and heating to 95 °C for 3 min. 2× SDS-PAGE loading buffer (100 μl) was added, and samples were reheated to 95 °C for 1 min. After brief centrifugation to remove glass beads, supernatants were collected, and duplicate samples were subjected to SDS-PAGE (7.5% acrylamide) and electrophoretic transfer to PVDF membranes. The membranes was probed with rabbit anti-Sec9 antibody (50) or rabbit anti-Kin2 antibody (18) followed by goat anti-rabbit HRP secondary antibodies and enhanced chemiluminescent detection.

Statistical analyses

Quantified peptide kinase assay and MRM data are shown as the means ± S.D. in cases where $n \geq 3$. Individual data points are shown for all quantified data, including experiments where $n = 2$.

Yeast growth assays

The indicated yeast strains were grown to midlogarithmic phase in either YPD (nontransformed) or SD-Ura (cells transformed with Kin2-expressing plasmids). Aliquots (2 μl) of a 5-fold dilution series (highest density $A_{600} = 0.5$) were spotted onto agar plates containing the indicated concentrations of tunicamycin, which were grown at 30 °C for 48–72 h. For experiments examining tunicamycin sensitivity of Kin2 mutants, a portion of the culture was retained to prepare cell lysates for immunoblotting. The cells (10 A_{600} units) were collected by centrifugation, washed with double-distilled H_2O, repelleted, flash frozen in liquid N_2, and stored at −80 °C. Cell lysates for immunoblots were prepared by mechanical disruption and TCA precipitation as described (51) in a total volume of 1 ml of extraction buffer. The protein pellet was suspended in 150 μl of 100 mM Tris HCl, pH 11.0, and 3% SDS and heated to boiling for 5 min. Following centrifugation, 120 μl of the supernatant was combined with 40 μl of 4× SDS-PAGE loading buffer and reheated to boiling. Following SDS-PAGE (7.5% acrylamide) and transfer to PVDF membrane, immunoblotting was performed with anti-GFP (600-101-215; Rockland) and anti-HCS (31F5; Santa Cruz) antibodies. The samples were visualized on an LiCor Odyssey CLx using fluorophore-conjugated secondary antibodies.

Author contributions—G. R. J., C. I. H., P. B., and B. E. T. conceptualization; G. R. J., H. J. L., C. I. H., and P. B. resources; G. R. J., H. J. L., K. W., C. I. H., M. D., P. B., and B. E. T. investigation; G. R. J., H. J. L., K. W., C. I. H., M. D., P. B., and B. E. T. methodology; G. R. J., K. W., C. I. H., P. B., and B. E. T. writing-review and editing; P. B. and B. E. T. supervision; P. B. and B. E. T. funding acquisition; K. W. and B. E. T. visualization; K. W. and B. E. T. writing-original draft.

Acknowledgments—We thank Erol Gulcicek, Chris Colangelo, Thomas Abbott, and Lisa Chung (Yale Keck Proteomics Resource) for targeted MS analysis of Sec9 phosphorylation; Philip Kim (University of Toronto) for compiling the list of previously identified yeast phosphorylation sites used for this study; Martin Schmidt (University of Pittsburgh) for sharing recombinant Elm1 kinase; and Michael Snyder (Stanford University) for sharing plasmids and strains.

References

1. Hornbeck, P. V., Kornhauser, J. M., Tkachev, S., Zhang, B., Skrzypek, E., Murray, B., Latham, V., and Sullivan, M. (2012) PhosphoSitePlus: a comprehensive resource for investigating the structure and function of experimentally determined post-translational modifications in man and mouse. *Nucleic Acids Res.* **40,** D261–D270 CrossRef Medline
2. Miller, C. J., and Turk, B. E. (2018) Homing in: mechanisms of substrate targeting by protein kinases. *Trends Biochem. Sci.* **43,** 380–394 CrossRef Medline
3. Cesaro, L., and Pinna, L. A. (2015) The generation of phosphoserine stretches in phosphoproteins: mechanism and significance. *Mol. Biosyst.* **11,** 2666–2679 CrossRef Medline
4. Yaffe, M. B. (2002) Phosphotyrosine-binding domains in signal transduction. *Nat. Rev. Mol. Cell Biol.* **3,** 177–186 CrossRef Medline
5. Reinhardt, H. C., and Yaffe, M. B. (2013) Phospho-Ser/Thr-binding domains: navigating the cell cycle and DNA damage response. *Nat. Rev. Mol. Cell Biol.* **14,** 563–580 CrossRef Medline
6. Kõivomägi, M., Ord, M., Iofik, A., Valk, E., Venta, R., Faustova, I., Kivi, R., Balog, E. R., Rubin, S. M., and Loog, M. (2013) Multisite phosphorylation networks as signal processors for Cdk1. *Nat. Struct. Mol. Biol.* **20,** 1415–1424 CrossRef Medline
7. Fiol, C. J., Mahrenholz, A. M., Wang, Y., Roeske, R. W., and Roach, P. J. (1987) Formation of protein kinase recognition sites by covalent modification of the substrate. Molecular mechanism for the synergistic action of casein kinase II and glycogen synthase kinase 3. *J. Biol. Chem.* **262,** 14042–14048 Medline

8. Dajani, R., Fraser, E., Roe, S. M., Young, N., Good, V., Dale, T. C., and Pearl, L. H. (2001) Crystal structure of glycogen synthase kinase 3β: structural basis for phosphate-primed substrate specificity and autoinhibition. *Cell* **105,** 721–732 CrossRef Medline
9. Frame, S., Cohen, P., and Biondi, R. M. (2001) A common phosphate binding site explains the unique substrate specificity of GSK3 and its inactivation by phosphorylation. *Mol. Cell* **7,** 1321–1327 CrossRef Medline
10. Cho, W. H., Lee, Y. J., Kong, S. I., Hurwitz, J., and Lee, J. K. (2006) CDC7 kinase phosphorylates serine residues adjacent to acidic amino acids in the minichromosome maintenance 2 protein. *Proc. Natl. Acad. Sci. U.S.A.* **103,** 11521–11526 CrossRef Medline
11. Lasa-Benito, M., Marin, O., Meggio, F., and Pinna, L. A. (1996) Golgi apparatus mammary gland casein kinase: monitoring by a specific peptide substrate and definition of specificity determinants. *FEBS Lett.* **382,** 149–152 CrossRef Medline
12. Chen, S., Jiang, X., Gewinner, C. A., Asara, J. M., Simon, N. I., Cai, C., Cantley, L. C., and Balk, S. P. (2013) Tyrosine kinase BMX phosphorylates phosphotyrosine-primed motif mediating the activation of multiple receptor tyrosine kinases. *Sci. Signal.* **6,** ra40 Medline
13. Begley, M. J., Yun, C. H., Gewinner, C. A., Asara, J. M., Johnson, J. L., Coyle, A. J., Eck, M. J., Apostolou, I., and Cantley, L. C. (2015) EGF-receptor specificity for phosphotyrosine-primed substrates provides signal integration with Src. *Nat. Struct. Mol. Biol.* **22,** 983–990 CrossRef Medline
14. Hunter, T. (2007) The age of crosstalk: phosphorylation, ubiquitination, and beyond. *Mol. Cell* **28,** 730–738 CrossRef Medline
15. Serber, Z., and Ferrell, J. E., Jr. (2007) Tuning bulk electrostatics to regulate protein function. *Cell* **128,** 441–444 CrossRef Medline
16. Levin, D. E., Hammond, C. I., Ralston, R. O., and Bishop, J. M. (1987) Two yeast genes that encode unusual protein kinases. *Proc. Natl. Acad. Sci. U.S.A.* **84,** 6035–6039 CrossRef Medline
17. Lamb, A., Tibbetts, M., and Hammond, C. I. (1991) The product of the KIN1 locus in *Saccharomyces cerevisiae* is a serine/threonine-specific protein kinase. *Yeast* **7,** 219–228 CrossRef Medline
18. Donovan, M., Romano, P., Tibbetts, M., and Hammond, C. I. (1994) Characterization of the KIN2 gene product in *Saccharomyces cerevisiae* and comparison between the kinase activities of $p145^{KIN1}$ and $p145^{KIN2}$. *Yeast* **10,** 113–124 CrossRef Medline
19. Tassan, J. P., and Le Goff, X. (2004) An overview of the KIN1/PAR-1/MARK kinase family. *Biol. Cell* **96,** 193–199 CrossRef Medline
20. Moravcevic, K., Mendrola, J. M., Schmitz, K. R., Wang, Y. H., Slochower, D., Janmey, P. A., and Lemmon, M. A. (2010) Kinase associated-1 domains drive MARK/PAR1 kinases to membrane targets by binding acidic phospholipids. *Cell* **143,** 966–977 CrossRef Medline
21. Elbert, M., Rossi, G., and Brennwald, P. (2005) The yeast par-1 homologs kin1 and kin2 show genetic and physical interactions with components of the exocytic machinery. *Mol. Biol. Cell* **16,** 532–549 CrossRef Medline
22. Yuan, S. M., Nie, W. C., He, F., Jia, Z. W., and Gao, X. D. (2016) Kin2, the budding yeast ortholog of animal MARK/PAR-1 kinases, localizes to the sites of polarized growth and may regulate septin organization and the cell wall. *PLoS One* **11,** e0153992 CrossRef Medline
23. La Carbona, S., and Le Goff, X. (2006) Spatial regulation of cytokinesis by the Kin1 and Pom1 kinases in fission yeast. *Curr. Genet.* **50,** 377–391 CrossRef Medline
24. La Carbona, S., Allix, C., Philippe, M., and Le Goff, X. (2004) The protein kinase kin1 is required for cellular symmetry in fission yeast. *Biol. Cell* **96,** 169–179 CrossRef Medline
25. Drewes, G., and Nurse, P. (2003) The protein kinase kin1, the fission yeast orthologue of mammalian MARK/PAR-1, localises to new cell ends after mitosis and is important for bipolar growth. *FEBS Lett.* **554,** 45–49 CrossRef Medline
26. Cadou, A., La Carbona, S., Couturier, A., Le Goff, C., and Le Goff, X. (2009) Role of the protein kinase Kin1 and nuclear centering in actomyosin ring formation in fission yeast. *Cell Cycle* **8,** 2451–2462 CrossRef Medline
27. Cadou, A., Couturier, A., Le Goff, C., Soto, T., Miklos, I., Sipiczki, M., Xie, L., Paulson, J. R., Cansado, J., and Le Goff, X. (2010) Kin1 is a plasma membrane-associated kinase that regulates the cell surface in fission yeast. *Mol. Microbiol.* **77,** 1186–1202 CrossRef Medline
28. Levin, D. E., and Bishop, J. M. (1990) A putative protein kinase gene ($kin1^+$) is important for growth polarity in *Schizosaccharomyces pombe*. *Proc. Natl. Acad. Sci. U.S.A.* **87,** 8272–8276 CrossRef Medline
29. Anshu, A., Mannan, M. A., Chakraborty, A., Chakrabarti, S., and Dey, M. (2015) A novel role for protein kinase Kin2 in regulating HAC1 mRNA translocation, splicing, and translation. *Mol. Cell. Biol.* **35,** 199–210 CrossRef Medline
30. Lee, M. E., Rusin, S. F., Jenkins, N., Kettenbach, A. N., and Moseley, J. B. (2018) Mechanisms connecting the conserved protein kinases Ssp1, Kin1, and Pom1 in fission yeast cell polarity and division. *Curr. Biol.* **28,** 84–92.e4 CrossRef Medline
31. Mok, J., Kim, P. M., Lam, H. Y., Piccirillo, S., Zhou, X., Jeschke, G. R., Sheridan, D. L., Parker, S. A., Desai, V., Jwa, M., Cameroni, E., Niu, H., Good, M., Remenyi, A., Ma, J. L., *et al.* (2010) Deciphering protein kinase specificity through large-scale analysis of yeast phosphorylation site motifs. *Sci. Signal.* **3,** ra12 Medline
32. Dale, S., Wilson, W. A., Edelman, A. M., and Hardie, D. G. (1995) Similar substrate recognition motifs for mammalian AMP-activated protein kinase, higher plant HMG-CoA reductase kinase-A, yeast SNF1, and mammalian calmodulin-dependent protein kinase I. *FEBS Lett.* **361,** 191–195 CrossRef Medline
33. Bodenmiller, B., Campbell, D., Gerrits, B., Lam, H., Jovanovic, M., Picotti, P., Schlapbach, R., and Aebersold, R. (2008) PhosphoPep: a database of protein phosphorylation sites in model organisms. *Nat. Biotechnol.* **26,** 1339–1340 CrossRef Medline
34. Gerber, S. A., Rush, J., Stemman, O., Kirschner, M. W., and Gygi, S. P. (2003) Absolute quantification of proteins and phosphoproteins from cell lysates by tandem MS. *Proc. Natl. Acad. Sci. U.S.A.* **100,** 6940–6945 CrossRef Medline
35. Picotti, P., Bodenmiller, B., Mueller, L. N., Domon, B., and Aebersold, R. (2009) Full dynamic range proteome analysis of *S. cerevisiae* by targeted proteomics. *Cell* **138,** 795–806 CrossRef Medline
36. Nešić, D., Miller, M. C., Quinkert, Z. T., Stein, M., Chait, B. T., and Stebbins, C. E. (2010) *Helicobacter pylori* CagA inhibits PAR1-MARK family kinases by mimicking host substrates. *Nat. Struct. Mol. Biol.* **17,** 130–132 CrossRef Medline
37. Goodwin, J. M., Svensson, R. U., Lou, H. J., Winslow, M. M., Turk, B. E., and Shaw, R. J. (2014) An AMPK-independent signaling pathway downstream of the LKB1 tumor suppressor controls Snail1 and metastatic potential. *Mol. Cell* **55,** 436–450 CrossRef Medline
38. Parsons, A. B., Brost, R. L., Ding, H., Li, Z., Zhang, C., Sheikh, B., Brown, G. W., Kane, P. M., Hughes, T. R., and Boone, C. (2004) Integration of chemical-genetic and genetic interaction data links bioactive compounds to cellular target pathways. *Nat. Biotechnol.* **22,** 62–69 CrossRef Medline
39. Sarno, S., Vaglio, P., Marin, O., Issinger, O. G., Ruffato, K., and Pinna, L. A. (1997) Mutational analysis of residues implicated in the interaction between protein kinase CK2 and peptide substrates. *Biochemistry* **36,** 11717–11724 CrossRef Medline
40. Tagliabracci, V. S., Engel, J. L., Wen, J., Wiley, S. E., Worby, C. A., Kinch, L. N., Xiao, J., Grishin, N. V., and Dixon, J. E. (2012) Secreted kinase phosphorylates extracellular proteins that regulate biomineralization. *Science* **336,** 1150–1153 CrossRef Medline
41. Xiao, J., Tagliabracci, V. S., Wen, J., Kim, S. A., and Dixon, J. E. (2013) Crystal structure of the Golgi casein kinase. *Proc. Natl. Acad. Sci. U.S.A.* **110,** 10574–10579 CrossRef Medline
42. Uboha, N. V., Flajolet, M., Nairn, A. C., and Picciotto, M. R. (2007) A calcium- and calmodulin-dependent kinase Ialpha/microtubule affinity regulating kinase 2 signaling cascade mediates calcium-dependent neurite outgrowth. *J. Neurosci.* **27,** 4413–4423 CrossRef Medline
43. Bachmann, M., Hennemann, H., Xing, P. X., Hoffmann, I., and Möröy, T. (2004) The oncogenic serine/threonine kinase Pim-1 phosphorylates and inhibits the activity of Cdc25C-associated kinase 1 (C-TAK1): a novel role for Pim-1 at the G_2/M cell cycle checkpoint. *J. Biol. Chem.* **279,** 48319–48328 CrossRef Medline
44. Scrimale, T., Didone, L., de Mesy Bentley, K. L., and Krysan, D. J. (2009) The unfolded protein response is induced by the cell wall integrity

mitogen-activated protein kinase signaling cascade and is required for cell wall integrity in *Saccharomyces cerevisiae*. *Mol. Biol. Cell* **20,** 164–175 CrossRef Medline

45. Gelperin, D. M., White, M. A., Wilkinson, M. L., Kon, Y., Kung, L. A., Wise, K. J., Lopez-Hoyo, N., Jiang, L., Piccirillo, S., Yu, H., Gerstein, M., Dumont, M. E., Phizicky, E. M., Snyder, M., and Grayhack, E. J. (2005) Biochemical and genetic analysis of the yeast proteome with a movable ORF collection. *Genes Dev.* **19,** 2816–2826 CrossRef Medline
46. Rice, L. M., Brennwald, P., and Brünger, A. T. (1997) Formation of a yeast SNARE complex is accompanied by significant structural changes. *FEBS Lett.* **415,** 49–55 CrossRef Medline
47. Lee, Y. J., Jeschke, G. R., Roelants, F. M., Thorner, J., and Turk, B. E. (2012) Reciprocal phosphorylation of yeast glycerol-3-phosphate dehydrogenases in adaptation to distinct types of stress. *Mol. Cell. Biol.* **32,** 4705–4717 CrossRef Medline
48. Cherry, J. M., Hong, E. L., Amundsen, C., Balakrishnan, R., Binkley, G., Chan, E. T., Christie, K. R., Costanzo, M. C., Dwight, S. S., Engel, S. R., Fisk, D. G., Hirschman, J. E., Hitz, B. C., Karra, K., Krieger, C. J., *et al.* (2012) Saccharomyces Genome Database: the genomics resource of budding yeast. *Nucleic Acids Res.* **40,** D700–D705 CrossRef Medline
49. Elbing, K., McCartney, R. R., and Schmidt, M. C. (2006) Purification and characterization of the three Snf1-activating kinases of *Saccharomyces cerevisiae*. *Biochem. J.* **393,** 797–805 CrossRef Medline
50. Brennwald, P., Kearns, B., Champion, K., Keränen, S., Bankaitis, V., and Novick, P. (1994) Sec9 is a SNAP-25-like component of a yeast SNARE complex that may be the effector of Sec4 function in exocytosis. *Cell* **79,** 245–258 CrossRef Medline
51. Cox, J. S., Chapman, R. E., and Walter, P. (1997) The unfolded protein response coordinates the production of endoplasmic reticulum protein and endoplasmic reticulum membrane. *Mol. Biol. Cell* **8,** 1805–1814 CrossRef Medline